JACS
JOURNAL OF THE AMERICAN CHEMICAL SOCIETY

Article

pubs.acs.org/JACS

Cell-Based Proteome Profiling of Potential Dasatinib Targets by Use of Affinity-Based Probes

Haibin Shi,[†,‡] Chong-Jing Zhang,[†,‡] Grace Y. J. Chen,[†] and Shao Q. Yao*[,†,‡]

[†]Department of Chemistry and [‡]NUS MedChem Program of the Life Sciences Institute, 3 Science Drive 3, National University of Singapore, Singapore 117543

Supporting Information

ABSTRACT: Protein kinases (PKs) play an important role in the development and progression of cancer by regulating cell growth, survival, invasion, metastasis, and angiogenesis. Dasatinib (BMS-354825), a dual Src/Abl inhibitor, is a promising therapeutic agent with oral bioavailability. It has been used for the treatment of imatinib-resistant chronic myelogenous leukemia (CML). Most kinase inhibitors, including Dasatinib, inhibit multiple cellular targets and do not possess exquisite cellular specificity. Recent efforts in kinase research thus focus on the development of large-scale, proteome-wide chemical profiling methods capable of rapid identification of potential cellular (on- and off-) targets of kinase inhibitors. Most existing approaches, however, are still problematic and in many cases not compatible with live-cell studies. In this work, we have successfully developed a cell-permeable kinase probe (**DA-2**) capable of proteome-wide profiling of potential cellular targets of Dasatinib. In this way, highly regulated, compartmentalized kinase−drug interactions were maintained. By comparing results obtained from different proteomic setups (live cells, cell lysates, and immobilized affinity matrix), we found **DA-2** was able to identify significantly more putative kinase targets. In addition to Abl and Src family tyrosine kinases, a number of previously unknown Dasatinib targets have been identified, including several serine/threonine kinases (PCTK3, STK25, eIF-2A, PIM-3, PKA C-α, and PKN2). They were further validated by pull-down/immunoblotting experiments as well as kinase inhibition assays. Further studies are needed to better understand the exact relevance of Dasatinib and its pharmacological effects in relation to these newly identified cellular targets. The approach developed herein should be amenable to the study of many of the existing reversible drugs/drug candidates.

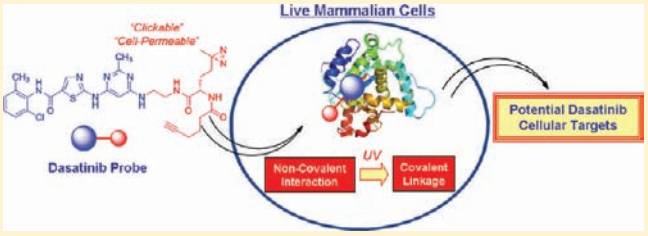

INTRODUCTION

Protein kinases (PKs) play a key role in signal transduction and regulate a variety of cellular processes. Dysregulation of kinase activities is implicated in many human diseases including cancer.[1] Consequently, of the 500+ known PKs in humans, many are considered potential therapeutic targets.[2] For example, the Src family nonreceptor tyrosine kinases (including Src, Lck, Hck, Fyn, Blk, Lyn, Fgr, Yes, and Yrk) are present in essentially all metazoan cells, where they have been reported to control a myriad of cellular processes including proliferation, migration, invasion, and survival.[3] Clinical studies have shown that Src is correlated with malignant progression of human tumors and thus is a promising therapeutic target.[4] Another example is the Bcr-Abl tyrosine kinase, which is constitutively activated in chronic myelogenous leukemia (CML) and drives the proliferation of stem cells in the bone marrow, thus causing the resulting pathology of the disease.[5] The remarkable success of Imatinib (an FDA-approved drug for the treatment of CML by selectively targeting Bcr-Abl)[5b] underscores the enormous potential of other kinase inhibitors in the drug discovery pipeline from major pharmaceutical companies.[6] Dasatinib, also known as BMS-354825 and sold under the trade name Sprycel by Bristol-Myers Squibb, is another drug that is a dual Bcr-Abl and Src family tyrosine kinase inhibitor.[7] This drug has already been approved by FDA for treatment of Imatinib-resistant CML and is also being evaluated for use in numerous other cancers such as advanced prostate and breast cancer.[8]

Despite intensive research efforts in recent years, most kinase inhibitors developed thus far, including those that are already on the market (i.e., Imatinib and Dasatinib), tend to inhibit multiple cellular targets and do not possess the type of exquisite cellular specificity that one typically desires in an ideal drug. This is because most kinase inhibitors target the ATP-binding site of the enzyme, which is highly conserved even among different classes of kinases. As a result, they have many potential cellular off-targets.[5b] In rare cases like Imatinib and Dasatinib, where side effects of the drugs are tolerable, they were able to pass through the stringent clinical trials and eventually make it to the market. In most other cases, they were rejected without undergoing further development.[5−7] In order to better understand the cellular selectivity of kinase inhibitors and to anticipate potential side effects of these drug candidates at the earliest stages of their development, recent efforts in kinase research have undergone a paradigm shift by focusing on the development of large-scale, proteome-wide chemical profiling

Received: September 9, 2011
Published: January 13, 2012

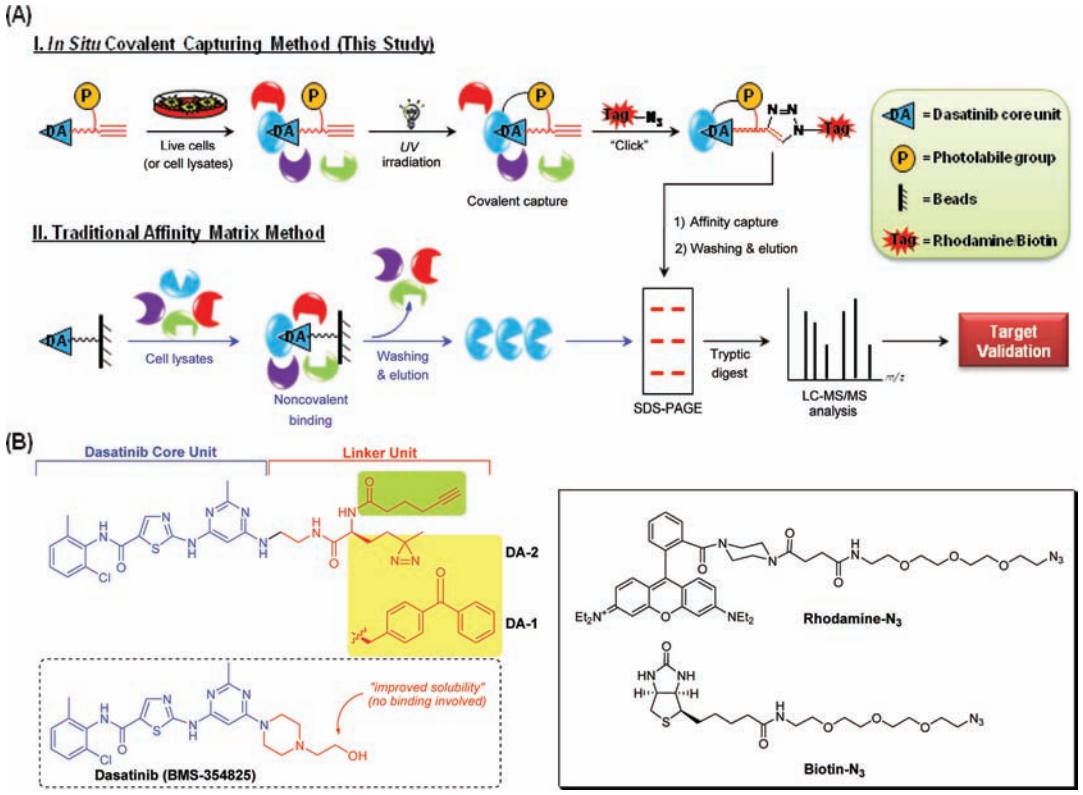

Figure 1. (A) Comparison of our newly developed, in situ covalent capturing method (top) and existing traditional affinity matrix method (bottom[12]) for large-scale, proteome-wide identification of kinase–drug interaction. In the traditional method, immobilized kinase "baits" were used to noncovalently capture kinases present in cellular lysates. In our in situ covalent method, a cell-permeable probe was used, which first went into cells and noncovalently bound to its cellular targets. Upon UV irradiation, the noncovalent probe–target interaction was converted to covalent binding. The cells were subsequently lysed, clicked with a suitable reporter, and then profiled (by in-gel fluorescence scanning) or affinity-enriched, followed by SDS–PAGE/LCMS for target identification. (B) The two affinity-based probes (AfBPs), **DA-1** and **DA-2**, used in this study. Apart from the linker unit (in red), which contains a photo-cross-linker and a terminal alkyne, they were otherwise structurally identical to Dasatinib (boxed below). The two click reporters (rhodamine-N_3 and biotin-N_3; boxed on the right) were previously reported.[14a].

methods capable of rapid identification of potential cellular (on- and off-) targets of kinase inhibitors.[9] Moving away from the traditional kinase screening method, which relies on in vitro kinase activity assays by screening the drug candidate against a panel of recombinantly purified, predetermined kinases,[10] newer screening methods cover significantly more kinases in the human kinome and endeavor to carry out kinase–drug screening under native cellular settings as much as possible.[11−13] For example, Fabian et al.[11] made use of a panel of 119 kinases expressed as a fusion to T7 bacteriophage and a small set of immobilized kinase probes to profile 20 kinase inhibitors. Upon being attached onto a phage particle, the kinase was rendered amplifiable, making it easy to handle, and the approach is extremely sensitive and amenable to large-scale applications. The obvious drawbacks, however, are that some kinases were not able to retain their full enzymatic activities on the phage surface and that conditions used in screening the phage-bound, kinase–drug interaction were hardly cell-like. Affinity purification methods combined with mass spectrometry (MS) in recent years have also found wide applications in large-scale profiling of kinome–drug interactions.[12] In order to study kinase–drug interactions under native cellular settings, the drug of interest may be directly added to cells and initiate binding to its intended targets. Upon cell lysis, immobilized kinase probes were added to the cell lysates, as "baits", to capture endogenous kinases present in the lysates. By measuring the amount of a kinase captured on beads by quantitative MS, with and without drug treatment, this method was able to reliably profile kinase–drug interactions in cells indirectly.[12c,d] Related methods developed by Superti-Furgo and co-workers[12e,f] used resin-immobilized probes, modified from drugs of interest, to directly capture and profile potential kinase binders present in cellular lysates. However, most of these approaches are still problematic in several important aspects. First, the heavy reliance on a small number of bead-immobilized kinase baits (which affects the accessibility of some target kinases) inevitably leads to "missed targets" by excluding many of the 500+ kinases from being studied. Second, the use of cellular lysates instead of live cells at some stages of the experimental process means that highly regulated, endogenous kinase expression levels, which vary greatly in different cellular compartments, are not sufficiently accounted for during kinase–drug interactions. Last, due to the non-covalent interaction between the bait and the kinase, relatively mild washing conditions must be applied, which often leads to accumulation of "false positives", as well as exclusion of weaker kinase–drug interactions.[9] To alleviate some of these issues, a kinase inhibitor-derived, trifunctional probe that can target kinases by the formation of kinase–drug complexes in solution was recently developed.[13] The need for a photo-cross-linker and a biotin affinity tag concurrently in the kinase inhibitor core, however, rendered this probe too bulky to enter cells. It is therefore not compatible with live-cell studies either. Our long-term research aim has been to develop chemical strategies

dx.doi.org/10.1021/ja208518u | J. Am. Chem. Soc. 2012, 134, 3001−3014

Scheme 1. Synthesis of DA-1 and DA-2

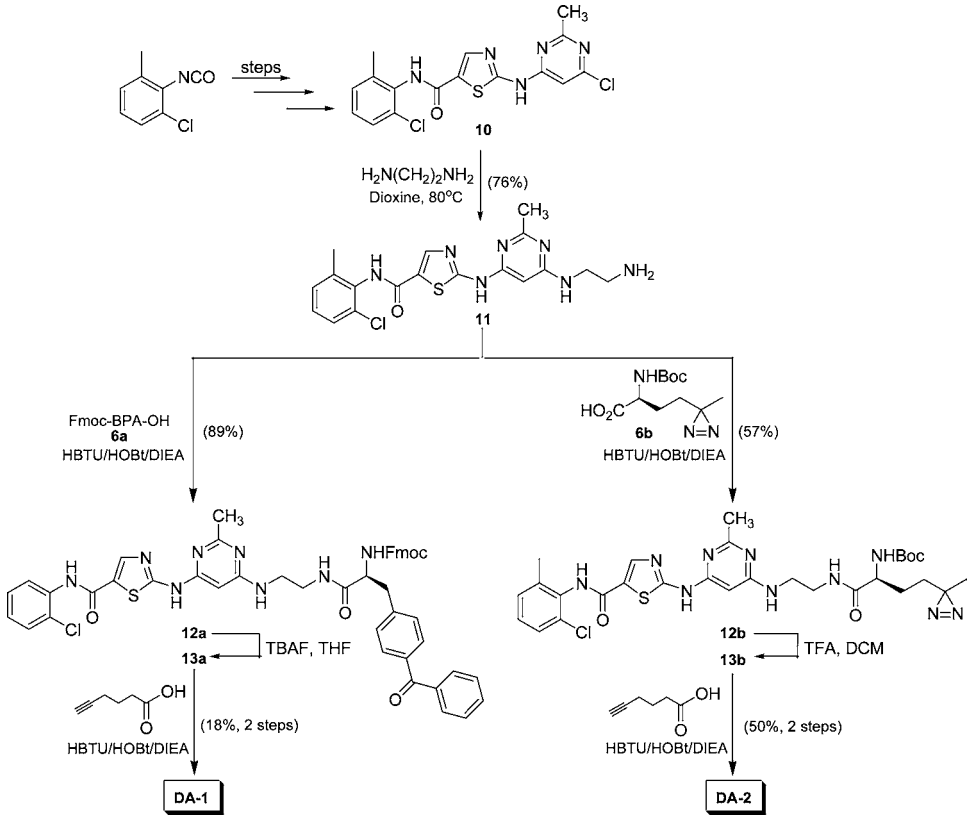

capable of interrogating protein−drug interactions under native cellular environments (in live cells, not cell lysates),[14] and in the context of kinase research, this calls for the design of small molecule probes that are cell-permeable, minimally disrupt kinase−drug interactions, and effectively capture interacting cellular targets in situ.[14c,d] Herein, we have successfully developed a cell-permeable kinase probe (**DA-2**) capable of proteome-wide profiling of potential cellular targets of Dasatinib (Figure 1). We have used **DA-2** to compare pull-down/liquid chromatography−mass spectrometry (LCMS) results from both cellular lysates (in vitro) and live-cell (in situ) experiments. Furthermore, by comparing with results obtained from Dasatinib-immobilized affinity matrix under similar experimental settings, we have confirmed that this photo-cross-linking approach is much more effective for the identification of kinase−drug interactions. Throughout the course of this study, several unknown cellular targets of Dasatinib have been successfully identified for the first time and further validated by standard biochemical assays (pull-down/immunoblotting and kinase inhibition assays).

RESULTS AND DISCUSSION

Design and Synthesis of Dasatinib Probes DA-1 and DA-2. Unlike our previously developed probes based on Olistat (a covalent antiobesity drug marketed under the trade name Xenical by Roche),[14a] Dasatinib is a reversible kinase inhibitor that binds the kinase ATP site noncovalently. Therefore, a drastically different approach was needed in order to profile Dasatinib−kinase interactions in live cells. Specifically, in our probe design, careful considerations were made to maintain the integrity of these noncovalent interactions and at the same time convert them in situ into stable covalent linkages suitable for downstream proteomic profiling and pull-down/target identification.[9] We took a cue from the field of activity-based protein profiling (ABPP),[15] in which covalent affinity-based probes (AfBPs) targeting different enzymes have been developed (Figure 1A).[16] Our two AfBPs based on Dasatinib, **DA-1** and **DA-2**, as shown in Figure 1B, have three essential structural components: (1) Dasatinib's pyrimidine core (in blue), which retains virtually all of the drug's original kinase-binding elements; (2) a photoreactive moiety, which in our case is either a benzophenone (for **DA-1**) or an alkyl diazirine (for **DA-2**), in place of the hydroxyethylpiperazinyl moiety in Dasatinib, which was previously shown to impart only the drug's solubility and may be modified without appreciable loss of kinase inhibitory activity;[17] (3) a small terminal alkyne handle, which would be used for subsequent ex vivo pull-down/target identification by conjugation to suitable reporters (rhodamine-N_3 or biotin-N_3; boxed in Figure 1B) via the bioorthogonal click chemistry.[18] Based on our previous experience, the choice of the photo-cross-linker and the alkyne handle was critical in keeping the overall probe small (MW < 800 Da) and cell-permeable, in order to ensure the covalent kinase−probe linkage takes place and to faithfully mimic the noncovalent kinase−drug interaction inside live cells.[14c,d] A deliberate effort was therefore made to design the smallest linker unit available for **DA-1** and **DA-2** (in red; Figure 1B). Previously designed kinase probes having a directly attached fluorophore tend to have significantly reduced inhibitory properties and poor cell permeability, with rare exceptions, and therefore were not suitable for live-cell studies and to report true cellular kinase−drug interactions.[19] We also noted that structural motifs such as the hydroxyethylpiperazinyl group in Dasatinib (which do not normally participate in protein−

dx.doi.org/10.1021/ja208518u | J. Am. Chem. Soc. 2012, 134, 3001−3014

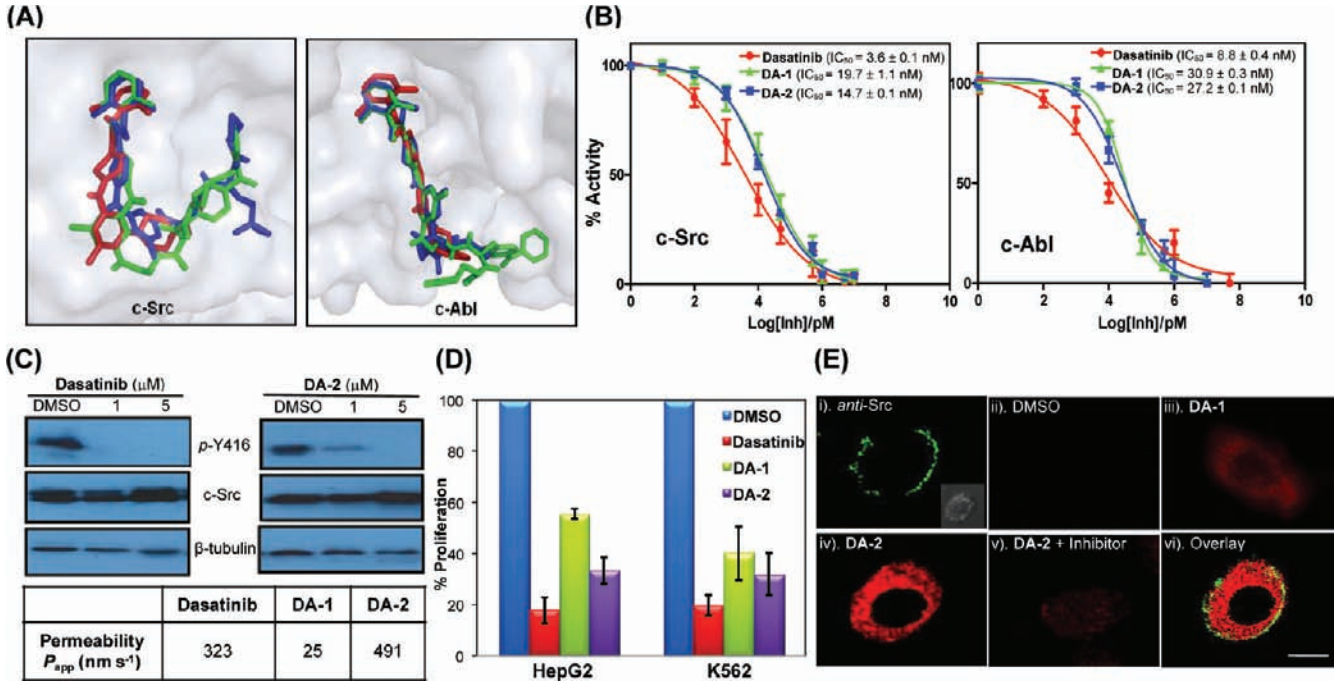

Figure 2. (A) Molecular docking of **DA-1** and **DA-2** in the ATP-binding pocket of c-Src and c-Abl kinase domains. Dasatinib, **DA-1**, and **DA-2** are shown in red, green and blue, respectively. (B) IC_{50} plots and corresponding values of Dasatinib, **DA-1**, and **DA-2** against purified c-Src and c-Abl kinase domains as determined by Kinase-Glo Plus luminescent assay. (C) Western blotting analysis showing dose-dependent inhibition of autophosphorylation at Tyr^{416} of c-Src transiently transfected in CHOK1 mammalian cells, with Dasatinib (left) and **DA-2** (right). For p-Y416, blots were detected with an antibody that specifically detects only the Y416-phosphorylated form of c-Src. For c-Src, blots were detected with anti-c-Src pan antibody. For β-tubulin, blots were probed with anti-tubulin antibody, as loading controls. Cell permeability results of the compounds are shown below. (D) Antiproliferative results of HepG2 and K562 cells treated with 20 μM Dasatinib, **DA-1**, and **DA-2** (72-h treatment), as determined by XTT assay. (E) Cellular imaging results of live HepG2 cells probed with 20 μM **DA-1** and **DA-2** (5-h treatment; colored in red). Immunofluorescence (IF) was performed with anti-c-Src antibody (colored in green). For the competitive experiment (panel iv), cells were first incubated with 50 μM Dasatinib for 30 min, prior to labeling with **DA-2**. (vi) overlay of panels i and iv. All images were acquired in the same way. Scale bar = 10 μm.

drug interactions) are common features in many drugs/drug candidates.[2,6] They are thus compatible with our above design principle as well.

Synthesis of the two "clickable" Dasatinib probes is shown in Scheme 1. Compound **10** was synthesized from the commercially available 1-chloro-2-isocyanato-3-methylbenzene following previously published methods (see Scheme S1 in the Supporting Information).[17a] Next, it was reacted with 1,2-diaminoethane in dioxane under reflux conditions to afford **11** (80% yield). Subsequent coupling reaction between **11** and either the commercially available Fmoc-protected benzophenone (**6a**) or the Boc-protected diazirine (**6b**, prepared in-house from glutamic acid in six steps; see Supporting Information), gave **12a** and **12b**, respectively. Finally, deprotection of the amine groups, followed by coupling with hex-5-ynoic acid, gave the two Dasatinib probes, **DA-1** and **DA-2** (18% and 50% yield, respectively, in two steps).

Molecular Modeling and Determination of IC_{50} Values. Dasatinib is a potent Src/Abl inhibitor with low nanomolar inhibition against both Bcr-Abl and c-Src, as well as several other Src family nonreceptor tyrosine kinases (e.g., Lck, and Yes).[17a] Recent large-scale chemical proteomic studies have also shown that it is able to inhibit a number of other related kinases, including Btk, Csk, Tec, EGFR, etc.[11b,12] Since the X-ray structures of the kinase domains for both c-Src (PDB ID 2SRC)[20] and c-Abl (PDB ID 2GQG)[21] complexed to Dasatinib are available, we carried out molecular docking experiments with our probes in order to gain better insights into their bindings to these two kinases (Figure 2A).[22] The docking results confirmed that the Dasatinib core in both **DA-1** and **DA-2** bound expectedly to the ATP-binding pocket of both c-Src and c-Abl in a manner that was closely matched to that of the drug itself, indicating that our benzophenone/diazirine-alkyne linker units in the two probes were a suitable replacement for the hydroxyethylpiperazinyl moiety in Dasatinib. Careful inspection of the structures further revealed a crucial pair of hydrogen bonds was formed between the hydroxyl oxygen of the gatekeeper residue Thr^{338} in c-Src (Thr^{315} in c-Abl) within the hinge region of the kinase's ATP pocket and the carbonyl oxygen of the thiazole amide in the two probes, which is consistent with the reported X-ray structure of Abl/Dasatinib complex.[21] As expected, the linker unit in both **DA-1** and **DA-2** appeared to be projected toward the solvent-exposed surface of the two kinases, thus resulting in little or no interference with the kinase−drug interaction.

Next, we performed in vitro kinase inhibition assay with recombinantly purified c-Src and c-Abl kinase domains using a standard Kinase-Glo Plus luminescence assay. Both **DA-1** and **DA-2** were tested together with Dasatinib (Figure 2B); under our assay conditions, the observed IC_{50} values of the two probes against c-Src were 19.7 ± 1.1 nM for **DA-1** and 14.7 ± 0.1 nM for **DA-2**, which were slightly higher than that of Dasatinib itself (3.6 ± 0.1 nM). Similarly, for c-Abl inhibition, the IC_{50} values of **DA-1** (30.9 ± 0.3 nM) and **DA-2** (27.2 ± 0.1 nM) also indicated that they were nearly as potent as Dasatinib

dx.doi.org/10.1021/ja208518u | J. Am. Chem. Soc. 2012, 134, 3001−3014

(8.8 ± 0.4 nM). These results thus indicate that both probes were good mimics of Dasatinib.

Effects on Autophosphorylation of c-Src and Cell Proliferation. While both probes were able to potently inhibit the c-Src/c-Abl kinase domains, we wondered if similar effects could be observed with the full-length (Fl) kinases expressed in mammalian cells. Bcr-Abl tyrosine kinase is an oncogenic fusion protein that is ∼210 kDa in size and cannot be easily handled.[21] On the other hand, the full-length c-Src is much smaller (∼60 kDa) and has been extensively studied in molecular biology.[23] Consequently for convenience, most of our experiments in the present work were carried out with c-Src. We first determined the cell permeability of the two probes (Figure 2C; bottom); results indicated **DA-2** was at least as cell-permeable as Dasatinib with a P_{app} value of 491 nm·s^{-1}, while **DA-1** was comparably less cell-permeable (P_{app} = 25 nm·s^{-1}). Therefore only **DA-2** was subsequently used for most other cell-based experiments. The full-length c-Src kinase contains several domains in addition to the tyrosine kinase domain (SH1 domain): an SH2 domain, an SH3 domain, an N-terminal variable region that could be both myristoylated and palmitoylated, and a flexible tyrosine-containing C-terminal tail. It has been known that the C-terminal tail tyrosine phosphorylation (at Tyr^{527}) by another kinase called Csk (C-terminal Src kinase) negatively regulates the tyrosine kinase activity of c-Src, while the autophosphorylation of Tyr^{416} located in the SH1 domain stimulates c-Src tyrosine kinase activity.[23] Inhibition of Tyr^{416} autophosphorylation in the full-length c-Src therefore serves as a convenient means to test Dasatinib's cellular inhibitory effects.[12d,23] Full-length c-Src was transiently expressed in CHOK1 mammalian cells. Upon treatment with different doses of Dasatinib and **DA-2** (0, 1, and 5 μM), a significant reduction of Tyr^{416} autophosphorylation in c-Src, but not its total protein expression, was observed (Figure 2C). We further evaluated the antiproliferative activities of the probes in HepG2 and K562 mammalian cell lines (these cell lines are routinely used to study cellular effects of Dasatinib).[12] As shown in Figure 2D, following 72-h probe treatment, both Dasatinib and **DA-2** showed good antiproliferative activities against both cell lines, with Dasatinib showing a higher potency. **DA-1** on the other hand showed the weakest antiproliferative activities, possibly due to its poor cell permeability. Again, our cell-based results on these two probes indicate **DA-2** is indeed a cell-permeable probe that may reasonably report Dasatinib−kinase interactions in live cells.

Cellular Imaging with DA-2. There has been enormous interest in the development of small-molecule-based imaging probes capable of reporting in vivo enzymatic activities.[24] Compartmentalization of live-cell-compatible probes has been shown to affect their intended cellular targets.[25] In a very recent example, Weissleder and co-workers[26] reported a bioorthogonal small molecule probe [derived from the Polo-like kinase 1 (PLK1) inhibitor BI2536] that could be used to image PLK1 in live cells. While it was not our original intention to develop small-molecule kinase imaging probes, we realized immediately that **DA-2**, by virtue of its excellent cell permeability and biochemical/cellular activities, may serve as a useful imaging probe to detect endogenous "Dasatinib-responsive" kinase activities (e.g., Src/Abl family tyrosine kinases). Since Dasatinib is known to target a number of other Src/Abl family kinases besides c-Src and Bcr-Abl, **DA-2** was therefore not expected to be a c-Src/Bcr-Abl specific imaging probe. Live HepG2 cells were used in our imaging experiments. First, the cells were treated with **DA-2** for 5 h (<10% cell death was observed at the end of probe treatment), followed by UV irradiation to initiate covalent kinase−probe linkage. Subsequently, cells were fixed, permeabilized, treated with rhodamine-N_3 following our previously optimized click chemistry protocols,[14a] and then imaged (Figure 2E). For cells treated with **DA-2**, strong fluorescence signals were observed throughout the whole cell excluding the nucleus (panel iv), and most were readily competed away by pretreatment with Dasatinib (panel v), indicating they originated from specific bindings between **DA-2** and Dasatinib-responsive kinases. Immunofluorescence (IF) was performed on the same cells by use of an anti-c-Src pan antibody (which detects all forms of c-Src), which indicated the cellular localization of endogenous c-Src expression was mostly membrane-bound (panel i). No fluorescence was observed in cells treated with dimethyl sulfoxide (DMSO) alone. Weak fluorescence was detected in cells treated with **DA-1**, again confirming this probe has comparatively poorer cell permeability and cellular activities. These results thus indicate that **DA-2** was a suitable imaging probe to detect endogenous cellular activities of c-Src (membrane-bound) and other "Dasatinib-responsive" proteins.

In Vitro Labeling with Purified Kinases. We first assessed whether **DA-2** serves as an effective AfBP for covalent labeling of Dasatinib-binding kinases in vitro. Recombinant c-Src and c-Abl kinase domains were used. Dose-dependent experiments were carried out by varying the concentration of the kinase in the labeling reaction. Following UV irradiation and click chemistry with rhodamine-N_3,[14a] the samples were separated by sodium dodecyl sulfate−polyacrylamide gel electrophoresis (SDS−PAGE) and visualized by in-gel fluorescence scanning (Figure 3A); as expected, proportional increases in the fluorescence intensity of labeled bands were observed with increasing concentrations of the kinases. As little as ∼1 pmol of c-Src/c-Abl could be detected, indicating the high affinity of **DA-2** for these two kinases.

As mentioned earlier, Tyr^{416} and Tyr^{527} phosphorylations in c-Src serve as positive and negative regulators of its kinase activities via intricate interactions among various domains of this kinase.[23] However, mutations at both residues, as previously shown, were not expected to cause any structural deformation in the ATP-binding pocket of the kinase domain.[20] Mutations in the gatekeeper residue Thr^{338} of c-Src, on the other hand, are well-known to result in structural changes in the kinase ATP site and cause resistance to Dasatinib.[27] For example, the T338 M mutant of c-Src, in which the gatekeeper residue in the hinge region of the ATP pocket is exchanged for a larger hydrophobic residue Met, was shown to cause a steric clash that impedes the binding of ATP-competitive inhibitors.[27a] In order to make an effective AfBP and to accurately report Dasatinib−kinase cellular interactions, **DA-2** should be able to distinguish between the active and "deformed" ATP pockets of c-Src. To prove this, we expressed and purified four different mutants of c-Src kinase domain (residues 251−533, containing the C-terminal tail), which were conveniently named Y416C, Y527C, Y416CY527C (a double mutant), and T338M, and we labeled them with **DA-2** (Figure 3B). Only the T338 M mutation of c-Src failed to be successfully labeled by **DA-2**, presumably due to its "deformed" ATP pocket. The other three mutants were shown to be labeled by **DA-2** as efficiently as the wild-type c-Src (lanes 1−4 in Figure 3B). Finally, competitive labeling was performed with different amounts of staurosporine, a well-known ATP-competitive

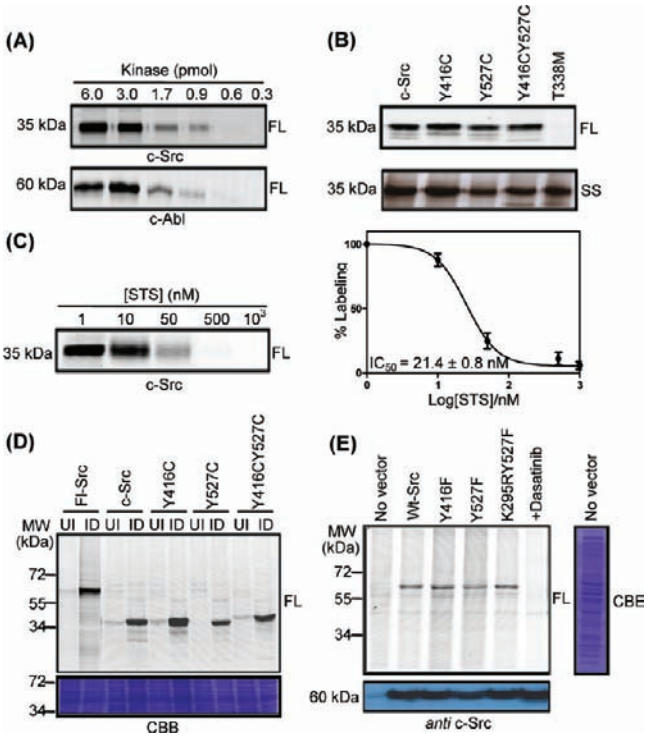

Figure 3. Labeling of c-Src (as well as c-Abl) and its various mutants by **DA-2**. In-gel fluorescence scanning was carried out as described in Materials and Methods. (A) Concentration-dependent labeling of purified c-Src/c-Abl (kinase domain) by **DA-2** (1 μM). (B) Labeling of c-Src (kinase domain) and its four mutants (Y416C, Y527C, Y416CY527C, and T338M) by **DA-2** (1 μM). Protein concentration = 100 nM. FL = fluorescent gel. SS = silver-stained gel, indicating equal loading of total proteins. (C) Dose-dependent inhibition of **DA-2**/c-Src labeling (**DA-2** = 1 μM; c-Src kinase domain = 100 nM) by staurosporine (STS) and the corresponding IC_{50} plot (right). % Labeling is the relative fluorescence of the labeled kinase in the presence of inhibitor (100% = no inhibitor). IC_{50} of STS was calculated from the plot to be 21.4 ± 0.8 nM. (D) Fluorescence labeling profiles of induced (ID) and uninduced (UI) bacteria expressing full-length (Fl)-Src, the kinase domain of c-Src, and its three mutants by **DA-2** (1 μM). (E) Labeling profiles of CHOK1 lysates transiently transfected with wild-type (Wt) c-Src and its three mutants by **DA-2** (1 μM). Dasatinib-competitive experiment was shown in lane 5. CBB: Coomassie brilliant blue-stained gel of lane 1.

general inhibitor of kinases (Figure 3C); results showed a dose-dependent inhibition in c-Src labeling with a calculated IC_{50} value of 21.4 ± 0.8 nM, which is similar to what was reported previously.[28] All these lines of evidence indicate that **DA-2** is a good mimic of Dasatinib and could potentially be used to quantitatively distinguish subtle structural changes in the ATP pocket of c-Src/c-Abl, as well as their binding availability in real cellular settings.

Labeling of c-Src in Bacterial and Mammalian Proteomes. We next assessed whether **DA-2** could selectively label c-Src present in complex cellular proteomes. *Escherichia coli* lysates containing both the full-length (Fl-Src) and various mutants of kinase domain of c-Src (Y416C, Y527C, Y416CY527C) were collected and directly labeled by **DA-2** (Figure 3D). Uninduced cell lysates were similarly labeled as controls. Similarly, mammalian expression constructs of full-length c-Src (labeled as Wt-Src in Figure 3E) and its three mutants (Y416F, Y527F, and K295RY527F, most of which are catalytically inactive mutants of c-Src but all of which retain full ATP-binding capacity)[29] were transiently transfected in CHOK1 cells, and the resulting mammalian cell lysates were labeled by **DA-2** (Figure 3E). The fluorescent profiles of both the bacterial and mammalian proteomes clearly showed positive and highly specific labeling of the various Src mutants by **DA-2** (based on their ATP-binding pockets as earlier shown in Figure 3B), with minimal background labeling of other proteins. No labeling was observed in either the uninduced bacterial lysates or the untransfected mammalian lysates (lane 1 in Figure 3E). Finally, c-Src labeling in the mammalian proteome was completely blocked by pretreatment of the cell lysate with Dasatinib, again recapitulating our earlier hypothesis about **DA-2** and its ability to faithfully report Dasatinib−kinase interactions in cells.

Endogenous Proteome Labeling and Pull-Down/LCMS/Target Identification of DA-2 in Cell Lysates and Live Cells. Finally, we performed endogenous proteome labeling of **DA-2** against both cellular lysates and live cells of K562 and HepG2 cancer cell lines, followed by large-scale pull-down/LCMS experiments in an effort to identify potential cellular targets of Dasatinib. Equally important, we hoped to compare results obtained from different proteomic setups (live cells, cell lysates, and immobilized affinity matrix). Due to the cell-permeable, clickable nature of **DA-2**, this probe could be directly used, without any modification, in both live-cell and cell lysate experiments. For live-cell experiments, as shown in Figure 1A (top), grown cells were first incubated with **DA-2** to initiate the probe internalization and binding to its cellular targets. Subsequent UV irradiation converted the noncovalent probe−target interaction into a covalent linkage, which, once formed, would no longer be affected by external changes (i.e., decompartmentalization/concentration changes of proteins due to cell lysis), click chemistry, or subsequent pull-down processes. On the other hand, in the experiment with cell lysates, **DA-2** was directly incubated with cell lysates prior to UV irradiation. This method is similar to the one reported by Fischer et al.,[13] in which all cellular proteins were "pooled" together to freely interact with the probe. While it has been shown this method enables the pull-down of a greater number of potential proteins due to its nondiscrete nature, many of them may not be true cellular targets.[9,13a] This is because a true kinase−drug interaction in cells is determined not merely by the total cellular concentration of the kinase and the drug but, more importantly, by their subcellular localized concentrations where the actual interaction occurs.[9] Finally, in order to directly compare results from our two photo-cross-linking methods (in vitro and in situ) and those obtained from traditional immobilized affinity matrices (Figure 1A, bottom),[12] the corresponding Dasatinib affinity beads were prepared by coupling the compound directly to a commercially available hydrophilic Affi-Gel resin (Figure 4A), based on previously used methods.[12e] To ensure a fair comparison among different experiments, all subsequent labeling/pull-down/LCMS experiments were carried out under identical conditions, unless otherwise indicated.

We first optimized the labeling experiments with **DA-2** under in vitro (cell lysate) and in situ (live cell) settings (Figure 4B); it was shown that, for both K562 and HepG2 cells, 5-h treatment of the reaction with 10 and 20 μM **DA-2** at room temperature provided sufficient labeling in cell lysates and live-cell experiments, respectively. The conditions were also chosen to ensure that, under live-cell experiments, the problem of cell death caused by the drug treatment (in our case, **DA-2**) was

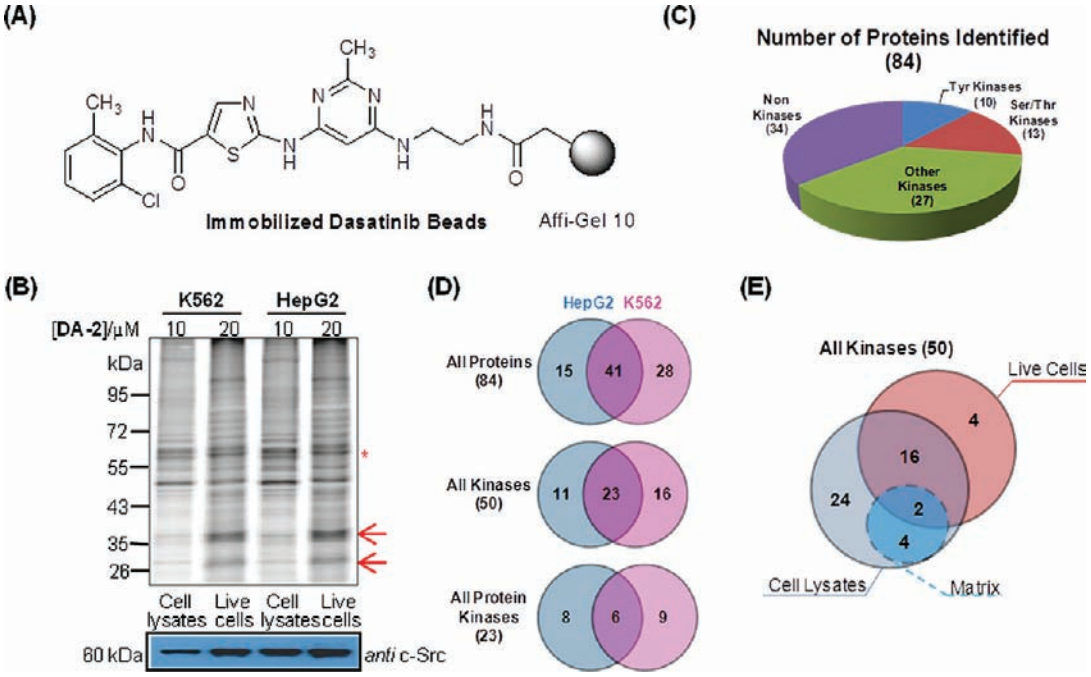

Figure 4. Summary of endogenous proteome pull-down/LCMS results from different methods. (A) Immobilized Dasatinib matrix used in our bead-based pull-down experiments. The beads are similar to those previously reported.[12e] (B) In vitro (cell lysates) and in situ (live cell) labeling profiles of K562 and HepG2 cells with **DA-2** (10 or 20 μM as indicated). The red asterisk marks the position corresponding to the fluorescently labeled endogenous c-Src, which was subsequently confirmed by pull-down/immunoblotting experiments (bottom gels). Arrows indicate representative fluorescent bands that showed different labeling profiles between in vitro and in situ experiments. (C) Pie chart summarizing the distribution of different proteins in the 84 putative Dasatinib targets identified from our experiments by **DA-2** (Table S1 in the Supporting Information). (D) Venn diagrams showing protein type-specific distributions of the putative Dasatinib targets identified from HepG2 (left, colored in blue) and K562 (right, colored in pink) cell lines. (E) Venn diagram analysis of the number of protein kinases identified from each of the three proteomic methods (in vitro, in situ, and immobilized Dasatinib matrix). A total of 50 kinases were identified from the three methods combined.

not significant (<10% cell death). In live-cell experiments, a higher concentration of **DA-2** was needed in order to achieve comparable labeling profiles, likely a reflection of the fact that it took longer for the probe to reach intended cellular targets. For both types of cells, although the in vitro and in situ labeling profiles were similar for the most part, obvious differences were evident (arrows in Figure 4B). For example, a 37-kDa protein band and a 26-kDa protein band were labeled strongly in the in situ experiment of both K562 and HepG2 cells (lanes 2 and 4) but were only weakly labeled in the in vitro experiment (lanes 1 and 3). These results further underscore our earlier hypothesis that, even with the same kinase probe (i.e., **DA-2**), different potential kinase targets may emerge from in vitro and in situ experiments. A large number of labeled bands were detected in all four lanes that could be readily competed away by treatment with excessive Dasatinib, indicating they were likely specific cellular targets of the drug. Also evident in these lanes was a strong 60-kDa fluorescently labeled band (marked with a red asterisk in Figure 4B), which was subsequently assigned to endogenous c-Src kinase from the corresponding pull-down/immunoblotting experiments carried out under similar conditions (biotin-N_3 instead of rhodamine-N_3 was used during the click chemistry step; in bottom gels of Figure 4B). Taken together, these data reaffirmed that **DA-2** was a cell-permeable probe that could be used to profile potential cellular targets of Dasatinib in live-cell environments.

Finally, large-scale pull-down/LCMS experiments were carried out to identify potential cellular targets of Dasatinib under the above optimized conditions. Similar experiments were performed with the immobilized Dasatinib matrix as shown in Figure 4A. The full list of proteins identified from different experiments is given in Table S1 (Supporting Information), with key findings summarized in Figure 4C–E. As in the case of most large-scale LCMS experiments,[9,12,13] a large number of proteins were identified from each LCMS run, many of which were "sticky" and/or highly abundant proteins. They were automatically removed (see Materials and Methods and Supporting Information). "False" hits that appeared in control pull-down/LCMS experiments (without **DA-2**) were further eliminated. Of the remaining proteins, we placed our focus on those proteins that might be related to kinase activities/interactions (kinases, potential kinase interacting partners, kinase-like proteins, etc). As shown in Figure 4C, 84 proteins were identified by **DA-2** to be possible Dasatinib targets. Among them, 10 were tyrosine kinases, 13 were serine/threonine kinases, 27 were non-protein kinases, and the remaining 34 proteins were non-kinase proteins. On the contrary, only six kinases were identified from pull-down/LCMS experiments performed under identical conditions with the immobilized Dasatinib matrix (Figure 4A). This is not surprising because in the previous study, where similar immobilized Dasatinib beads were used, Superti-Furgo and co-workers[12e] managed to pull down only a few kinases as well. In another recent study with a trifunctional Dasatinib probe containing a photo-cross-linker and a biotin affinity tag, 18 kinases and nine non-kinase proteins were identified.[13b] Our results thus confirm that, by using clickable probes over other resin-immobilized probes, compounds such as **DA-2** became much more accessible to their intended protein targets that may be potentially identified in pull-down/LCMS experiments. We

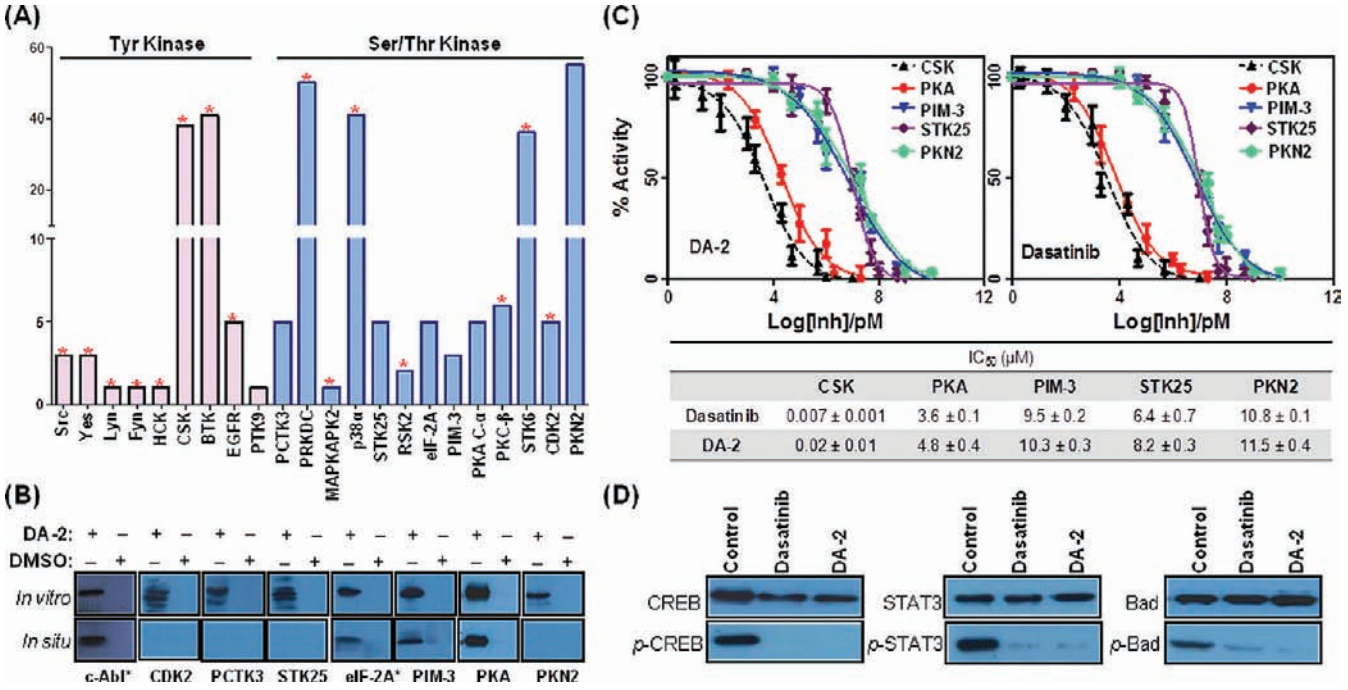

Figure 5. Validation of potential Dasatinib targets identified by use of **DA-2**. (A) Twenty-three protein kinases (10 tyrosine kinases and 13 serine/threonine kinases) identified from pull-down/LCMS experiments. The *y*-axis indicates the number of unique peptides obtained from LCMS data. See Table S1 in the Supporting Information for details. Previously reported Dasatinib targets are marked with an asterisk. (B) Target validation of selected kinases by use of both in vitro and in situ pull-down/immunoblotting experiments. Experiments were done with HepG cells, as well as K562 cells (labeled with asterisks). See Materials and Methods for details. For STAT3 validation, see Figure S1 in the Supporting Information. (C) IC_{50} inhibition plots (top) and summary (bottom) of recombinant domains of Csk, PKA, PIM-3, STK25, and PKN2 against **DA-2** (left graph) and Dasatinib (right graph). (D) Inhibition of the phosphorylation state of downstream signaling proteins (CREB, STAT3, and Bad) by Dasatinib and **DA-2** (24-h treatment) in K562 cells. Control indicates cells treated with DMSO only. Equal amounts of the resulting cell lysates were analyzed for CREB, STAT3, and Bad phosphorylation by Western blotting with antibodies specific for the native form of proteins and for residues that are phosphorylated (p-) in each protein. The concentration of Dasatinib and **DA-2** was 10 μM.

therefore argue that, in future proteomic experiments, small clickable probes such as **DA-2** should be used, whenever possible, in order to maximize target identification. We next analyzed the 84 proteins identified from our experiments in cell-type-, protein-type-, and experiment-specific manners (Figure 4D,E); 56 proteins were identified from HepG2 cells and 69 from K562 cells, of which 41 appeared in both cell lines. Of all 50 kinases identified, 34 were from HepG2 cells and 39 from K562 cells, of which 23 kinases were identified in both cell lines. Of all 23 protein kinases identified, 14 were from HepG2 cells and 15 from K562 cells, of which six protein kinases were identified in both cell lines. Our results herein are in good agreement with previous findings that kinome−drug interactions are cell-type-specific, due to differences in the endogenous kinase expression levels in different cells.[12,13] Finally, by focusing on the 50 kinases identified from our experiments, we were able to further compare results obtained from different proteomic setups (Figure 4E): in vitro experiments (**DA-2** + lysates) identified 46 kinases, of which six were also identified from bead-based experiments (immobilized matrix + lysates), and 18 were also identified from in situ experiments with (**DA-2** + live cells). Interestingly, four kinases were identified only in live-cell experiments but not in either lysate-based experiment. We thus concluded that probes such as **DA-2**, which are compatible with live-cell environments, could in the future provide unique insights into the cell-based profiling of kinase−drug interactions in a manner other existing approaches cannot.[9,12,13]

Target Validation. By using **DA-2**, we have thus far identified a total of 50 kinases that might be potential cellular targets of Dasatinib. Since it would have been a herculean effort to validate each of these targets, we decided to focus on the 23 protein kinases (Figure 5A); there were 10 tyrosine kinases (Bcr-Abl, two isoforms of Src, Lyn, Yes, Hck, Csk, Btk, EGFR, and PTK9) and 13 serine/threonine kinases (p38α, PRKDC, STK6, CDK2, and so on) identified. Other non-protein kinases identified in our experiments included lipid kinases, pyruvate kinases, and others. While almost all of the tyrosine family kinases in our list (except PTK9) had previously been identified, we noted that only seven of the 13 serine/thronine family kinases (MAPKAPK2, RSK2, p38α, PRKDC, STK6, CDK2, and PKC-β) were previously shown as Dasatinib targets.[12,13a] The other six serine/threonine kinases (PCTK3, STK25, eIF-2A, PIM-3, PKA C-α, and PKN2) were unknown targets of Dasatinib. To validate that they were true cellular targets of Dasatinib, we repeated the **DA-2** labeling experiments with both cellular lysates and live cells and carried out pull-down/immunoblotting experiments with the respective antibodies. Abl and CDK2, two protein kinases previously validated to be Dasatinib targets,[12,13a] were used as positive controls (Figure 5B). Results unequivocally confirmed that all six newly identified Dasatinib targets were successfully labeled by **DA-2** with either cellular lysates or live cells, and these results corroborated well with those obtained from our LCMS experiments. Several kinases, including CDK2, PCTK3, STK25, and PKN2, were positively labeled by **DA-2** only in cellular lysates, which was consistent with the LCMS results.

STAT3 protein, a well-known transcription factor and a non-kinase identified from our LCMS experiments, was also confirmed as a true cellular target of Dasatinib (Figure S1 in Supporting Information). Taken together, our results further indicated that, in addition to the Src family tyrosine kinases, serine/threonine kinases may be another important group of kinases that directly interact with Dasatinib. Next, we carried out kinase inhibition assays against most of the newly identified serine/threonine kinases with Dasatinib and **DA-2**. Five different recombinant kinases were tested, four of which were newly identified targets of Dasatinib (PKA, PIM-3, STK25, and PKN2). As shown in Figure 5C, for Csk (a previously known Dasatinib target), its IC_{50} values with Dasatinib and **DA-2** were 7.1 ± 0.3 nM and 20.7 ± 0.1 nM, respectively. On the other hand, **DA-2** (and Dasatinib) showed IC_{50} values of 4.8 ± 0.4 μM (3.6 ± 0.1 μM) against PKA, 10.3 ± 0.3 μM (9.5 ± 0.2 μM) against PIM-3, 8.2 ± 0.3 μM (6.4 ± 0.7 μM) against STK25, and 11.5 ± 0.4 μM (10.8 ± 0.1 μM) against PKN2. These results indicate that our probe was able to capture both strong and weak binders of the drug. The fact that most of our newly identified kinases are weak binders of Dasatinib probably also explains why they evaded previous investigations.[12,13] Finally, we assessed whether inhibition of some of these newly identified kinase targets of Dasatinib affects the phosphorylation state of their downstream proteins. The CREB pathway regulates a broad array of cellular responses by mediation of signals from numerous physiological stimuli. The activation of CREB-1 by phosphorylation at Ser^{133} is known to be controlled by PKA and several other kinases.[30] Similarly, the inhibition of PIM-3 was previously shown to negatively affect the phosphorylation of Ser^{112} in Bad (a proapoptotic member of the Bcl-2 family proteins)[31a] and of Tyr^{705} in STAT3 (a transcription factor).[31b] As shown in Figure 5D, treatment of K562 cells with both Dasatinib and **DA-2** caused nearly complete inhibition of phosphorylation of each of these proteins, but not their endogenous total protein expression level, indicating the cellular inhibition of their upstream kinases, presumably PKA and PIM-3, might have occurred. We caution, however, due to the highly complex nature of the cellular phosphoproteome network, that our results presented herein could not rule out the possible involvement of other kinases.

CONCLUSION

We have successfully synthesized a clickable, cell-permeable kinase probe capable of proteome-wide profiling of potential cellular targets of Dasatinib. Unlike previously developed approaches for large-scale studies of kinome–drug interactions,[9,12,13] our strategy was able to directly interrogate the interaction of Dasatinib with its potential cellular targets in their native cellular environments. In this way, highly regulated, compartmentalized kinase–drug interactions were maintained. We compared results obtained from different proteomic setups (live cells, cell lysates, and immobilized affinity matrix) and found that, under similar experimental settings, our clickable probe (**DA-2**) was able to identify significantly more putative kinase targets (both in vitro and in situ) over immobilized Dasatinib affinity matrix. In addition to Abl and Src family tyrosine kinases, a number of previously unknown Dasatinib targets have been identified. Most notably, six serine/threonine kinases (PCTK3, STK25, eIF-2A, PIM3, PKA C-α, and PKN2), were identified for the first time and validated by pull-down/immunoblotting experiments with the corresponding antibodies, as well as by kinase inhibition assays. For some of these new Dasatinib targets (e.g., PKA and PIM-3), inhibition of the phosphorylation state of their downstream protein targets was further evaluated. The potential of **DA-2** as an imaging probe was also explored. Whereas further studies are needed to better understand the exact relevance of Dasatinib and its pharmacological effects in relation to these newly identified cellular targets, our findings point to a likely scenario that these proteins might be potential off-targets of Dasatinib. It is also possible that the overall biological activities of Dasatinib might have originated from this drug's ability to inhibit both its known targets as well as some of these newly identified targets.[2] Our previous efforts in the study of in situ protein–drug interaction had focused on covalent drugs,[14a] which take up only a small fraction of all drugs currently on the market.[32] The approach developed herein should be amenable to the study of a much larger pool of reversible drugs. It thus brings us one step closer to our long-term research goal of profiling all protein–drug interactions in situ.[33]

MATERIALS AND METHODS

General Information. Dasatinib and staurosporine were purchased from Invitrogen. Tris(2-carboxyethyl)phosphine (TCEP) and the click chemistry ligand tris[(1-benzyl-1*H*-1,2,3-triazol-4-yl)methyl]amine (TBTA) were purchased from Sigma–Aldrich. Antibodies against c-Src (sc-8056), PKA (sc-903), PIM-3 (C-18), CDK2 (AN4.3), STK25 (E-5), PKN2 (C-6), CREB, and PCTK-3 (P-23) were purchased from Santa Cruz Biotechnology. Antibodies against c-Abl, eIF-2A, STAT3, Bad, p-CREB, p-STAT3, p-Bad, and p-Y416 c-Src (2101) were purchased from Cell Signaling Technologies (Beverly, MA). Antibody against β-tubulin (ab6046) was purchased from Abcam. Recombinant STK25, PIM-3, and PKN2 as well as their peptide substrates were purchased from SignalChem. All DNA plasmids were obtained as previously reported[28,34] or purchased from commercial sources from Addgene (www.addgene.org) or Origene (www.origene.com). All mutants were generated from the corresponding wild-type constructs by use of the QuickChange site-directed mutagenesis kit (Stratagene) following manuals provided by the vendor. IC_{50} determination against recombinant kinase domains (c-Src, Abl, Csk, STK25, PIM-3, PKN2, and PKA) was performed with the Kinase-Glo Plus luminescent assay kit (Promega), as previously described.[28] The corresponding peptide substrates (c-Src, KVEKIGEGTYGVVYK; Abl, EAIYAAPFAKKK; PKA, LRRASLG; Csk, KKKKEEIYFFF; PIM-3, KRRRLSSLRA; PKN2, KRREILSRRPSYR; STK25, MBP protein) were used. Cell-permeability assay was carried out, as previously described,[35] with MDCK (Madin-Darby canine kidney) cells and with caffeine and lucifer yellow as controls. Molecular docking experiments were carried out as previously described.[36] Cell proliferation assay was carried out as previously described with 72-h compound treatment,[14a] using the XTT colorimetric cell proliferation kit (Roche) following manufacturer's guidelines.

Recombinant Protein Expression and Purification. Recombinant c-Src (residues 251–533) and its mutants (SrcY416C, SrcY527C, SrcY416C527C, and SrcT338M), tagged with a His_6 tag at their N-termini, were expressed by use of a pET-28a vector (Novagen) in BL21(DE3) *E. coli* strain.[34] Briefly, the two plasmids containing the kinase (pET-28a) and the phosphatase (pCDFDuet) were cotransformed into *E. coli* BL21(DE3) cells and plated on Luria–Bertani (LB) agar with kanamycin (50 μg/mL)/streptomycin (50 μg/mL)

dx.doi.org/10.1021/ja208518u | *J. Am. Chem. Soc.* 2012, 134, 3001–3014

and grown overnight at 37 °C. The next day, colonies from the plate were resuspended in LB medium supplemented with kanamycin (50 μg/mL) and streptomycin (50 μg/mL). Cultures were grown to an OD_{600} of 1.2 at 37 °C and cooled for 1 h with shaking at 18 °C prior to induction for 16 h at 18 °C with 0.2 mM isopropyl β-D-thiogalactoside (IPTG). Cells were then harvested by centrifugation (10 min × 7000 rpm at 4 °C) and stored at −80 °C, or resuspended in chilled resuspension buffer (50 mM Tris, 500 mM NaCl, 5% glycerol, and 25 mM imidazole, pH 8.0) for immediate purification by immobilized metal affinity chromatography. An aliquot (10−20 mL) of the resuspension buffer was used per liter of culture volume. Resuspended pellets were lysed by sonication on ice. Cell debris was pelleted by centrifugation (13 000 rpm × 20 min, 4 °C) in 1.5-mL eppendorf tubes. Clear supernatant containing the soluble protein was incubated for 3 h with 0.5−1 mL of nickel−nitrilotriacetic acid (Ni-NTA) agarose beads (Qiagen, Germany) per liter of culture volume. All purification procedures were carried out on ice or at 4 °C. The purification column was equilibrated with 1 column volume of wash buffer (50 mM NaH_2PO_4, 300 mM NaCl, and 20 mM imidazole, pH 8.0) prior to loading. Flow-through was collected. The column was washed with washing buffer for 10 column volumes. Proteins were then eluted with a buffer (containing 50 mM NaH_2PO_4, 300 mM NaCl, and 500 mM imidazole, pH 8.0) in 1−2 mL fractions. Protein concentration of each fraction was determined by Bradford protein assay (Bio-Rad), and the purity of the eluants was analyzed by use of SDS−10% polyacrylamide gels.

Cell Culture and Western Blotting. Cell lines were obtained from the National Cancer Institute Developmental Therapeutics Program (NCI-60). HepG2 and CHOK1 cells were cultured in Dulbecco's modified Eagle medum (DMEM; Invitrogen, Carlsbad, CA) containing 10% heat-inactivated fetal bovine serum (FBS; Invitrogen), 100 units/mL penicillin, and 100 μg/mL streptomycin (Thermo Scientific) and maintained in a humidified 37 °C incubator with 5% CO_2. K562 cells were maintained in RPMI-1640 medium supplemented with 10% FBS and 100 units/mL penicillin and 100 μg/mL streptomycin. To generate protein lysates, cells were washed twice with cold phosphate-buffered saline (PBS), harvested with 1× trypsin or by use of a cell scraper, and collected by centrifugation. Cell pellets were then washed with PBS and lysed with *N*-(2-hydroxyethyl)piperazine-*N*′-2-ethanesulfonic acid (Hepes) buffer (25 mM Hepes, 150 mM NaCl, and 2 mM $MgCl_2$, pH 7.5) containing 0.1% NP-40. Protein concentration was determined by Bradford protein assay. For Western blotting experiments (before and after pull-down experiments), samples from HepG2 or K562 cells were resolved by SDS−polyacrylamide gels and transferred to poly(vinylidene difluoride) membranes. Membranes were then blocked with 3% bovine serum albumin (BSA) in TBST (0.05% Tween in Tris-buffered saline) for 1 h at room temperature. After blocking, membranes were incubated with the corresponding primary antibody for another hour. After incubation, membranes were washed with TBST (4 × 10 min) and then incubated with an appropriate secondary antibody. Finally, blots were washed again with TBST before being developed with SuperSignal West Dura Kit (Thermo Scientific).

Transient Transfection. The wild-type full-length c-Src construct (OriGene) and three mutant constructs, SrcY416F, SrcY527F, and SrcK295RY527F (Addgene), were transiently transfected with Endofectin transfect reagents (Genecopoeia) at 80% confluency in CHOK1 cells. After 8 h, the medium was changed to fresh growth medium. The cells were incubated for another 24 h at 37 °C with 5% CO_2. To obtain protein lysates, cells were washed twice with cold PBS and lysed by incubation with lysis buffer (25 mM Hepes, 150 mM NaCl, 2 mM $MgCl_2$, and 0.1% NP-40, pH 7.5) for 30 min on ice. Cells were then resuspended and collected by centrifugation. Protein concentration was determined by Bradford protein assay, and the expression levels of c-Src and its mutants were assessed by Western blotting with anti-c-Src pan antibody.

Live Cell Imaging. HepG2 cells were seeded in glass-bottom dishes (Mattek) and grown until 70−80% confluency. Cells were then treated with 0.5 mL of DMEM with 20 μM **DA-1**, **DA-2**, or DMSO. After 5 h, the medium was removed, and cells were gently washed twice with PBS, followed by UV irradiation (350 nm) for 10 min. The cells were subsequently fixed for 15 min at room temperature with 3.7% formaldehyde in PBS, washed twice with cold PBS again, and permeabilized with 0.1% Triton X-100 in PBS for 10 min. Cells were then blocked with 2% BSA in PBS for 30 min, washed twice with PBS, and then subsequently treated with a freshly premixed click chemistry reaction solution in a 100 μL volume (final concentrations of reagents: 1 mM $CuSO_4$, 1 mM TCEP, 100 μM TBTA, and 10 μM rhodamine-N_3 in PBS) for 2 h at room temperature with vigorous shaking. Cells were washed with PBS at least three times. For co-localization experiments, cells were further incubated with anti-c-Src pan antibody (1:100) for 1 h at room temperature (or overnight at 4 °C), washed twice with PBS, and then incubated with fluorescein isothiocyanate (FITC)-conjugated anti-mouse IgG (1:500) for 1 h, following by washing again. For the competitive experiment, cells were first incubated with 50 μM Dasatinib for 30 min, prior to labeling with **DA-2**. Imaging was done with the Leica TCS SP5X confocal microscope system equipped with Leica HCX PL APO 63×/1.20 W CORR CS, 405 nm diode laser, white laser (470−670 nm, with 1 nm increments, with eight channels AOTF for simultaneous control of eight laser lines, each excitation wavelength provides 1.5 mV), and a photomultiplier tube (PMT) detector ranging from 410 to 700 nm for steady-state fluorescence. Images were processed with Leica Application Suite Advanced Fluorescence (LAS AF).

In Vitro and In Situ Proteome Labeling. Labeling of recombinantly purified proteins (c-Src and c-Abl) with **DA-1**/**DA-2** was done similarly as in vitro proteome labeling experiments, based largely on previously published procedures with some modifications.[14] For in vitro proteome labeling, the probe was added to fresh cell lysates (50 μg) in 50 μL of Hepes buffer at a desired concentration. Unless indicated otherwise, samples were incubated for 30 min at room temperature and then UV-irradiated (350 nm) for 20 min. Four microliters of a freshly premixed click chemistry reaction cocktail in PBS (100 μM rhodamine-N_3 from 1 mM stock solution in DMSO, 0.1 mM TBTA from 2.4 mM freshly prepared stock solution in deionized water, 1 mM TCEP from 24 mM freshly prepared stock solution in deionized water, and 1 mM $CuSO_4$ from 24 mM freshly prepared stock solution in deionized water) was added. The reaction was further incubated for 2 h with gentle mixing, before being terminated by addition of prechilled acetone (0.5 mL; 30 min incubation at −20 °C). Precipitated proteins were subsequently collected by centrifugation (13 000 rpm × 10 min at 4 °C). The supernatant was discarded and the pellet was washed with 200 μL of prechilled methanol (2×). The protein pellets were then resuspended in 20 μL of 1× SDS-

loading buffer and heated for 10 min at 95 °C. Around 20 μg (per gel lane) of protein was separated by SDS−PAGE (10% gel) and then visualized by in-gel fluorescence scanning on a Typhoon 9410 variable mode imager scanner. For in situ labeling, cells were grown to 80−90% confluency in 24-well plates under conditions described above. The medium was removed, and cells were washed twice with cold PBS and then treated with 0.5 mL of the DMEM-containing probe (diluted from DMSO stocks whereby DMSO never exceeded 1% in the final solution). After 5 h of incubation at 37 °C/5% CO_2, the medium was aspirated, and cells were washed gently with PBS (2×) to remove excessive probe, followed by UV irradiation for 20 min on ice. The cells were trypsinized and pelleted by centrifugation. Eventually, the cell pellets were resuspended in PBS (50 μL), homogenized by sonication, and diluted to 1 mg/mL with PBS. All subsequent procedures were similar to those from in vitro experiments.

Pull-Down/LCMS for Target Identification and Subsequent Validation. For putative target identification from in vitro/in situ labeling experiments with **DA-2** in HepG2 and K562 cell lines, lysates/live cells were treated with the probe as described above, followed by click chemistry with biotin-N_3, pulled-down with avidin−agarose beads (Pierce), and separated by SDS−PAGE before either LCMS analysis (for target identification) or immunoblotting (for target validation). Briefly for in vitro pull-down experiments, cellular lysates (5 mg) were supplemented with 200 μL of 5× Hepes buffer (125 mM Hepes, 750 mM NaCl, and 10 mM $MgCl_2$, pH 7.5) and the final reaction volume was eventually adjusted to 1 mL with Milli-Q water. A solution of **DA-2** (final concentration 10 μM; from 10 μL of 1 mM stock solution in DMSO) was added, followed by incubation at 4 °C for 2 h. The reaction mixture was then UV-irradiated for 20 min before addition of biotin-N_3 under click conditions as earlier described. Upon acetone precipitation and resolubilization (in PBS with 0.1% SDS with brief sonication), the resuspended sample was incubated with avidin−agarose beads (100 μL/mg of protein) at 4 °C overnight. After centrifugation, the supernatant was removed. The beads were washed with 0.1% SDS once and PBS four times and then boiled in SDS loading buffer (2×) [200 mM Tris, 400 mM dithiothreitol (DTT), and 8% SDS, pH 6.8] for 15 min, before being separated by SDS−PAGE. For in situ pull-down experiments, **DA-2** (final concentration 20 μM) was directly added to live cells, followed by incubation for 5 h at 37 °C/5% CO_2. DMSO should never exceed 1% in the final solution. Next, the medium was aspirated, and cells were washed twice gently with PBS to remove the excessive probe. UV irradiation was next carried out for 20 min on ice. The cells were trypsinized and pelleted by centrifugation. Eventually, cell pellets were resuspended in PBS (50 μL), homogenized by sonication, and diluted to 1 mg/mL with PBS. The labeled lysates were then subjected to click reaction with biotin-N_3 and other subsequent processes, as described above. Negative control pull-down experiments were done with DMSO (in place of **DA-2**).

For experiments involving inhibition of the phosphorylation state of downstream signaling proteins (p-CREB, p-STAT3, and p-Bad) by Dasatinib and **DA-2**, K562 cells were treated with the compounds (final concentration 10 μM) for 24 h. Control cells were treated with DMSO only. Equal amounts of the resulting cell lysates were analyzed for CREB, STAT3, and Bad phosphorylation by Western blotting with antibodies specific for the native form of proteins and for residues that are phosphorylated (p-) in each protein.

For LC-MS/MS protein identification, above pull-down fractions were separated by SDS−10% polyacrylamide gels, followed by silver or Coomassie blue staining. Each lane was cut into multiple gel slices. Trypsin digestion was performed on each gel slice with an in-gel trypsin digestion kit (Pierce). Digested peptides were then extracted from the gel with 50% acetonitrile and 1% formic acid. Tryptic peptide extracts were evaporated by speedvac and reconstituted with 10 μL of 0.1% trifluoroacetic acid (TFA). The peptides were separated and analyzed on a Shimadzu UFLC system (Shimadzu, Japan) coupled to an LTQ-FT Ultra (Thermo Electron, Germany). Mobile phase A (0.1% formic acid in H_2O) and mobile phase B (0.1% formic acid in acetonitrile) were used to establish the 60 min gradient comprising 45 min of 5−35% B, 8 min of 35−50% B, and 2 min of 80% B, followed by re-equilibrating at 5% B for 5 min. Peptides were then analyzed on LTQ-FT with an Advance CaptiveSpray Source (Michrom BioResources) at an electrospray potential of 1.5 kV. A gas flow of 2 L/min, ion transfer tube temperature of 180 °C, and collision gas pressure of 0.85 m Torr were used. The LTQ-FT was set to perform data acquisition in the positive-ion mode as previously described,[37a] except that the m/z range of 350−1600 was used in the full MS scan. The raw data were converted to mgf format. The database search was performed with an in-house Mascot server (version 2.2.07, Matrix Science) with MS tolerance of 10 ppm and MS/MS tolerance of 0.8 Da. Two missed cleavage sites of trypsin were allowed. Carbamidomethylation (C) was set as a fixed modification, and oxidation (M) and phosphorylation (S, T, and Y) were set as variable modifications.[37b] LC-MS/MS results obtained from the above experiments (in vitro, in situ, and negative control with DMSO) were processed as shown below, and results are summarized in the Supporting Information (section 2). As in the case of most large-scale LCMS experiments,[12,13,37] a large number of proteins were identified from each LCMS run, many of which were "sticky" and/or highly abundant proteins. These were automatically removed. "False" hits that appeared in control pull-down/LCMS experiments (where DMSO was used in place of **DA-2**) were further eliminated. From this remaining list, we placed our focus on those proteins that might be related to kinase activities/interactions (kinases, potential kinase interacting partners, kinase-like proteins, etc). They were further identified and listed in the Supporting Information (Table S1).

Chemical Synthesis. All chemicals were purchased from commercial vendors and used without further purification, unless otherwise noted. Tetrahydrofuran (THF) was distilled over sodium/benzophenone and used immediately. Dichloromethane (DCM, CH_2Cl_2) was distilled over CaH_2. All nonaqueous reactions were carried out under nitrogen atmosphere in oven-dried glassware. Reaction progress was monitored by thin-layer chromatography (TLC) on precoated silica plates (Merck 60 F254, 250 μm thickness) and spots were visualized by ceric ammonium molybdate, basic $KMnO_4$, UV light, or iodine. ^1H NMR and ^{13}C NMR spectra were recorded on a Bruker model Advance 300 MHz spectrometer or Bruker model DPX-500 MHz NMR spectrometer. Chemical shifts are reported in parts per million (ppm) referenced with respect to appropriate internal standards or residual solvent peaks ($CDCl_3$ = 7.26 ppm, CD_3OD = 3.31 ppm, DMSO-d_6 = 2.50 ppm). ^1H NMR coupling constants (J) are reported in Hertz (Hz) and

dx.doi.org/10.1021/ja208518u | J. Am. Chem. Soc. 2012, 134, 3001−3014

multiplicity is indicated as follows: s (singlet), d (doublet), t (triplet), q (quartet), m (multiplet), br s (broad singlet), dd (doublet of doublet). Mass spectra were obtained on Shimadzu ion-trap time-of-flight mass spectrometry (IT-TOF-MS) or Shimadzu electrospray ionization mass spectrometry (ESI-MS) systems.

*2-({6-[(2-Aminoethyl)amino]-2-methylpyrimidin-4-yl}-amino)-N-(2-chloro-6-methylphenyl)thiazole-5-carboxamide (**11**).* Compound **10** (500 mg, 1.26 mmol), prepared from previously reported procedures,[17a] was suspended in dioxane (2 mL). Subsequently, 1,2-diaminoethane (8 mL) was added and the resulting mixture was heated at 90 °C overnight. Upon solvent evaporation, an aqueous potassium hydroxide solution (10 M) was added to adjust the pH of the solution to 9. The mixture was finally filtered and the resulting solid was washed with ether and dried, giving the desired product **11** as a yellow solid (400 mg; 76.2% yield). ^{1}H NMR (300 MHz, DMSO-d_6) δ 8.20 (s, 1H), 7.38−7.41 (m, 1H), 7.23−7.30 (m, 2H), 5.86 (s, 1H), 3.37 (s, 2H), 2.85 (s, 2H), 2.36 (s, 3H), 2.24 (s, 3H). ^{13}C NMR (75 MHz, DMSO-d_6) δ 18.69, 25.77, 41.12, 55.26, 83.71, 125.74, 127.34, 128.47, 129.36, 132.84, 133.94, 139.20, 141.28, 156.27, 160.38, 163.19, 163.60, 165.64. IT-TOF-MS: m/z [M + 1]$^+$ calcd 418.12; found 418.11.

*{3-(4-Benzoylphenyl)-1-[(2-{[6-({5-[(2-chloro-6-methylphenyl)carbamoyl]thiazol-2-yl}amino)-2-methylpyrimidin-4-yl]amino}ethyl)amino]-1-oxopropan-2-yl} (9H-Fluoren-9-yl)methylcarbamate (**12a**).* To a solution of 2-({[(9H-fluoren-9-yl)methoxy]carbonyl}amino)-3-(4-benzoylphenyl)-propanoic acid **6a** (270 mg, 0.55 mmol) were added coupling reagents 1-hydroxybenzotriazole (HOBt; 74 mg, 0.55 mmol), *O*-(benzotriazol-1-yl)-*N*,*N*,*N*′,*N*′-tetramethyluronium hexafluorophosphate (HBTU; 208 mg, 0.55 mmol), and diisopropylethylamine (DIEA; 141 mg, 1.1 mmol). Compound **11** (417 mg, 0.5 mmol) was then added to the above solution and the reaction was stirred at room temperature overnight. Subsequently, the reaction was quenched with water at 0 °C and extracted with a mixture of $CHCl_3$/methanol (10:1; 100 mL). The organic layer was washed with water, sodium bicarbonate solution, ammonium chloride solution, and brine, followed by concentration in vacuo and precipitation with hexane/EtOAc (1:1). Upon filtration, the desired product **12a** was collected as a solid (400 mg; 88.9%). ^{1}H NMR (300 MHz, DMSO-d_6) δ 11.41 (s, 1H), 9.88 (s, 1H), 8.22 (s, 2H), 7.84 (d, J = 7.2 Hz, 2H), 7.58−7.67 (m, 9H), 7.21−7.44 (m, 13H), 5.89 (s, 1H), 4.23−4.28 (m, 2H), 4.10−4.12 (m, 2H), 3.11−3.32 (m, 1H), 2.72−3.08 (m, 2H), 2.35 (s, 3H), 2.22 (s, 3H). IT-TOF-MS: m/z [M + 1]$^+$ calcd 891.28; found 891.26.

***DA-1*.** To a solution of compound **12a** (387 mg, 0.43 mmol) in *N*,*N*-dimethylformamide (DMF; 10 mL) was added tetrabutylammonium fluoride (TBAF; 1 M in THF, 1 mL), and the reaction was stirred for 0.5 h at room temperature. The reaction was monitored by LCMS. The product was used for the next step without further purification. To a solution of hex-5-ynoic acid (50 mg, 0.44 mmol) in DMF (10 mL) were added coupling reagents HBTU (179 mg, 0.47 mmol), HOBt (67 mg, 0.5 mmol), and DIEA (110 mg, 0.92 mmol). The resulting mixture was stirred for 0.5 h at room temperature and then added to the crude product obtained from the previous step. The resulting reaction was stirred overnight at room temperature. Upon being quenched with water (20 mL), the reaction was extracted with $CHCl_3$/methanol (10:1; 20 mL × 3), and the combined organic layer was concentrated, purified by flash chromatography (DCM:MeOH = 15:1) to give the desired product, **DA-1** (60 mg; 18.3% yield in two steps). ^{1}H NMR (300 MHz, DMSO-d_6) δ 11.37 (s, 1H), 9.82 (s, 1H), 8.12−8.16 (m, 3H), 7.61−7.68 (m, 5H), 7.40−7.52 (m, 2H), 7.38 (d, J = 8.1 Hz, 2H), 7.26−7.36 (m, 2H), 7.15 (br s, 1H), 5.85 (s, 1H), 3.15 (m, 1H), 2.70−2.84 (m, 1H), 2.71 (s, 1H), 2.34 (s, 3H), 2.22 (s, 3H), 2.13 (s, 2H), 1.96−1.98 (m, 2H), 1.52−1.57 (m, 2H), 1.23 (s, 1H), 0.85 (m, 1H). ^{13}C NMR (75 MHz, DMSO-d_6) δ 195.4, 171.4, 171.1, 165.3, 163.0, 162.7, 159.9, 143.4, 140.8, 138.8, 137.2, 135.0, 133.5, 132.4, 129.5, 129.3, 129.0, 128.5, 127.0, 84.0, 71.3, 53.6, 37.8, 34.0, 25.4, 24.2, 22.0, 18.3, 17.2, 13.9. IT-TOF-MS: m/z [M + 1]$^+$ calcd 763.26; found 763.24.

*{1-[(2-{[6-({5-[(2-Chloro-6-methylphenyl)carbamoyl]-thiazol-2-yl}amino)-2-methylpyrimidin-4-yl]amino}ethyl)-amino]-4-(3-methyl-3H-diazirin-3-yl)-1-oxobutan-2-yl} tert-Butylcarbamate (**12b**).* To a mixture of 2-[(*tert*-butoxycarbonyl)amino]-4-(3-methyl-3*H*-diazirin-3-yl)butanoic acid **6b** (180 mg, 0.7 mmol) and compound **11** (200 mg, 0.48 mmol) in DMF (15 mL) were added coupling reagents HOBt (105 mg, 0.78 mmol), HBTU (300 mg, 0.79 mmol), and DIEA (175 mg, 1.35 mmol). The reaction was stirred for 24 h at room temperature in the dark. Upon being quenched by water (50 mL), the mixture was filtered and the resulting solid was washed with water and ether and precipitated in $CHCl_3$/methanol (10:1), giving the desired product **12b** (190 mg, 57.6%). ^{1}H NMR (300 MHz, DMSO-d_6) δ 11.39 (s, 1H), 9.83 (s, 1H), 8.20 (s, 1H), 7.90 (s, 1H), 7.40 (d, J = 2.1 Hz, 1H), 7.22−7.38 (m, 2H), 7.12 (s, 1H), 6.84 (d, J = 7.5 Hz, 1H), 5.86 (s, 1H), 3.80 (s, 1H), 3.25 (m, 4H), 2.38 (s, 3H), 2.24 (s, 3H), 1.22−1.48 (m, 13 H), 0.95 (s, 3H). IT-TOF-MS: m/z [M + 1]$^+$ calcd 657.25; found 657.30.

***DA-2*.** To a solution of compound **12b** (188 mg, 0.28 mmol) in DCM (10 mL) at 0 °C was added TFA (10 mL) slowly. The resulting mixture was stirred at room temperature overnight. Upon solvent evaporation in vacuo, the residue was suspended in DMF (8 mL), followed by addition of hex-5-ynoic acid (56 mg, 0.5 mmol), DIEA (240 mg, 1.86 mmol), HOBt (60 mg, 0.44 mmol), and HBTU (162 mg, 0.42 mmol). The reaction was further stirred at room temperature in the dark overnight before being quenched by water (30 mL). Upon filtration, the solid was washed with water and ether and precipitated with $CHCl_3$/methanol (10:1), giving the desired product **DA-2** (91 mg; 50% yield in two steps). ^{1}H NMR (300 MHz, DMSO-d_6) δ 11.40 (s, 1H), 9.84 (s, 1H), 8.20 (s, 1H), 7.92−7.997 (m, 2H), 7.39 (d, J = 6.9 Hz, 1H), 7.23−7.28 (m, 2H), 7.13 (br s, 1H), 5.87 (s, 1H), 4.18−4.13 (m, 1H), 3.24−3.31 (m, 4H), 2.76 (s, 1H), 2.38 (s, 3H), 2.12−2.23 (m, 7H), 2.04 (s, 1H), 1.24−1.67 (m, 7H), 0.95 (s, 3H). ^{13}C NMR (75 MHz, DMSO-d_6) δ 172.0, 171.8, 165.63, 163.1, 160.3, 141.1, 139.1, 133.9, 132.8, 129.3, 128.5, 127.3, 125.8, 84.4, 71.7, 52.3, 39.0, 30.6, 26.8, 26.0, 25.7, 24.5, 19.6, 18.6, 17.7. IT-TOF-MS: m/z [M + 1]$^+$ calcd 651.24; found 651.25.

■ ASSOCIATED CONTENT

Ⓢ Supporting Information

Additional relevant experimental and synthetic procedures, spectral characterization of compounds, LCMS results, and complete references. This material is available free of charge via the Internet at http://pubs.acs.org.

■ AUTHOR INFORMATION

Corresponding Author

chmyaosq@nus.edu.sg

■ ACKNOWLEDGMENTS

Financial support was provided by the Ministry of Education (R-143-000-394-112), the Agency for Science, Technology and Research (R-143-000-391-305), and the National Medical Research Council (NMRC/1260/2010). We thank Dr. Newman Sze (NTU, Singapore) and Jigang Wang (NUS) for LCMS experiments and Dr. Hao Wu (NUS) for cell permeability assays.

■ REFERENCES

(1) Cohen, P. *Nat. Rev. Drug Discovery* **2002**, *1*, 309−315.
(2) Dancey, J.; Sausville, E. A. *Nat. Rev. Drug Discovery* **2003**, *2*, 296−313.
(3) Kim, L. C.; Song, L.-X.; Haura, E. B. *Nat. Rev. Clin. Oncol.* **2009**, *6*, 587−595.
(4) Irby, R. B.; Yeatman, T. J. *Oncogene* **2000**, *19*, 5636−5642.
(5) (a) Deininger, M. W. N.; Goldman, J. M.; Melo, J. V. *Blood* **2000**, *96*, 3343−3356. (b) Capdeville, R.; Buchdunger, E.; Zimmermann, J.; Matter, A. *Nat. Rev. Drug Discovery* **2002**, *1*, 493−502.
(6) Jaenne, P. A.; Gray, N.; Settleman, J. *Nat. Rev. Drug Discovery* **2009**, *8*, 709−723.
(7) Shah, N. P.; Tran, C.; Lee, F. Y.; Chen, P.; Norris, D.; Sawyers, C. L. *Science* **2004**, *305*, 399−401.
(8) (a) Weisberg, E; Manley, P. W.; Cowan-Jacob, S. W.; Hochhaus, A.; Griffin, J. D. *Nat. Rev. Cancer* **2007**, *7*, 345−356. (b) Nam, S.; Kim, D. W.; Cheng, J. Q.; Zhang, S. M.; Lee, J. H.; Buettner, R.; Mirosevich, J.; Lee, F. Y.; Jove, R. *Cancer Res.* **2005**, *65*, 9185−9189.
(9) Rix, U.; Superti-Furgo, G. *Nat. Chem. Biol.* **2009**, *5*, 616−624.
(10) (a) Davies, S. P.; Reddy, H.; Caivano, M.; Cohen, P. *Biochem. J.* **2000**, *351*, 95−105. (b) Bain, J.; McLauchlan, H.; Elliott, M.; Cohen, P. *Biochem. J.* **2003**, *371*, 199−204.
(11) (a) Fabian, M. A.; et al. *Nat. Biotechnol.* **2005**, *23*, 329−336. (b) Karaman, M. W.; et al. *Nat. Biotechnol.* **2008**, *26*, 127−132.
(12) (a) Knockaert, M.; Gray, N.; Damiens, E.; Chang, Y. -T.; Grellier, P.; Grant, K.; Fergusson, D.; Mottram, J.; Soete, M.; Dubremetz, K.-F. *Chem. Biol.* **2000**, *7*, 411−422. (b) Knockaert, M.; Wieking, K.; Schmitt, S.; Leost, M.; Grant, K. M.; Mottram, J. C.; Kunick, C.; Meijer, L. *J. Biol. Chem.* **2002**, *277*, 25493−25501. (c) Bantscheff, M.; et al. *Nat. Biotechnol.* **2007**, *25*, 1035−1044. (d) Du, J.; et al. *Nat. Biotechnol.* **2009**, *27*, 77−83. (e) Hantschel, O.; Rix, U.; Schmidt, U.; Burckstummer, T.; Kneidinger, M.; Schutze, G.; Colinge, J.; Bennett, K. L.; Ellmeier, W.; Valent, P.; Superti-Furgo, G. *Proc. Natl. Acad. Sci. U.S.A.* **2007**, *114*, 13283−13288. (f) Li, J. H.; Rix, U.; Fang, B.; Bai, Y.; Edwards, A.; Colinge, J.; Bennett, K. L.; Gao, J.; Song, L.; Eschrich, S.; Superti-Furgo, G.; Koomen, J.; Haura, E. B. *Nat. Chem. Biol.* **2010**, *6*, 291−299.
(13) (a) Fischer, J. J.; Graebner, O. Y.; Dalhoff, C.; Michaelis, S.; Schrey, A. K.; Ungewiss, J.; Andrich, K.; Jeske, D.; Kroll, F.; Glinski, M.; Sefkow, M.; Dreger, M.; Koester, H. *J. Proteome Res.* **2010**, *9*, 806−817. (b) Fischer, J. J.; Dalhoff, C.; Schrey, A. K.; Graebner neé Baessler, O. Y.; Michaelis, S.; Andrich, K.; Glinski, M.; Kroll, F.; Sefkow, M.; Dreger, M.; Koester, H. *J. Proteomics* **2011**, *75*, 160−168.
(14) (a) Yang, P.-Y.; Liu, K.; Ngai, M. H.; Lear, M. J.; Wenk, M. R.; Yao, S. Q. *J. Am. Chem. Soc.* **2010**, *132*, 656−666. (b) Ngai, M. H.; Yang, P.-Y.; Liu, K.; Shen, Y.; Wenk, M. R.; Yao, S. Q.; Lear, M. J. *Chem. Commun.* **2010**, *46*, 8335−8337. (c) Kalesh, K. A.; Sim, D. S. B.; Wang, J..; Liu, K.; Lin, Q. S.; Yao, S. Q. *Chem. Commun.* **2010**, *46*, 1118−1120. (d) Shi, H.; Cheng, X.-M.; Sze, S. K.; Yao, S. Q. *Chem. Commun.* **2011**, *47*, 11306−11308.
(15) (a) Evans, M. J.; Cravatt, B. F. *Chem. Rev.* **2006**, *106*, 3279−3301. (b) Uttamchandani, M.; Li, J.; Sun, H.; Yao, S. Q. *ChemBioChem* **2008**, *9*, 667−675. (c) Fonović, M; Bogyo, M. *Exp. Rev. Proteomics* **2008**, *5*, 721−730. (d) Heal, W. P.; Dang, T. H. T.; Tate, E. W. *Chem. Soc. Rev.* **2011**, *40*, 246−257.
(16) (a) Saghatelian, A.; Jessani, N.; Joseph, A.; Humphrey, M.; Cravatt, B. F. *Proc. Natl. Acad. Sci. U.S.A.* **2004**, *101*, 10000−10005. (b) Chan, E. W. S.; Chattopadhaya, S.; Panicker, R. C.; Huang, X.; Yao, S. Q. *J. Am. Chem. Soc.* **2004**, *126*, 14435−14446. (c) Liu, K.; Shi, H.; Xiao, H.; Chong, A. G. L.; Bi, X.; Chang, Y. T.; Tan, K.; Yada, R. Y.; Yao, S. Q. *Angew. Chem., Int. Ed.* **2009**, *48*, 8293−8297. (d) Fuwa, H.; Takahashi, Y.; Konno, Y.; Watanabe, N.; Miyashita, H.; Sasaki, M.; Natsugari, H.; Kan, T.; Fukuyama, T.; Tomita, T.; Iwatsubo, T. *ACS Chem. Biol.* **2007**, *2*, 408−418. (e) Shi, H.; Liu, K.; Xu, A.; Yao, S. Q. *Chem. Commun.* **2009**, 5030−5032.
(17) (a) Lombardo, L. J.; et al. *J. Med. Chem.* **2004**, *47*, 6658−6661. (b) Veach, D. R.; Namavari, M.; Pillarsetty, N.; Santos, E. B.; Beresten-Kochetkov, T.; Lambek, C.; Punzalan, B. J.; Antczak, C.; Smith-Jones, P. M.; Djaballah, H.; Clarkson, B.; Larson, S. M. *J. Med. Chem.* **2007**, *50*, 5853−5857.
(18) (a) Kolb, H. C.; Sharpless, K. B. *Drug Discovery Today* **2003**, *8*, 1128−1137. (b) Meldal, M.; Tornøe, C. W. *Chem. Rev.* **2008**, *108*, 2952−3015. (c) Sletten, E. M.; Bertozzi, C. R. *Angew. Chem., Int. Ed.* **2009**, *48*, 6974−6998. (d) Kalesh, K. A.; Shi, H.; Ge, J.; Yao, S. Q. *Org. Biomol. Chem.* **2010**, *8*, 1749−1762.
(19) (a) Cohen, M. S.; Hadjivassiliou, H.; Taunton, J. *Nat. Chem. Biol.* **2007**, *3*, 156−160. (b) Blair, J. A.; Rauh, D.; Kung, C.; Yun, C.-H.; Fan, Q.-W.; Rode, H.; Zhang, C.; Eck, M. J.; Weiss, W. A.; Shokat, K. M. *Nat. Chem. Biol.* **2007**, *3*, 229−238. (c) Yee, M.-C.; Fas, S. C.; Stohlmeyer, M. M.; Wandless, T. J.; Cimprich, K. A. *J. Biol. Chem.* **2005**, *280*, 29053−29059.
(20) Xu, W. Q.; Doshi, A.; Lei, M.; Eck, M. J.; Harrison, S. C. *Mol. Cell* **1999**, *3*, 629−638.
(21) Tokarski, J. S.; Newitt, J. A.; Chang, C. Y.; Cheng, J. D.; Wittekind, M.; Kiefer, S. E.; Kish, K.; Lee, F. Y.; Borzillerri, R.; Lombardo, L. *Cancer Res.* **2006**, *66*, 5790−5797.
(22) (a) Sanner, M. F. *J. Mol. Graphics Model.* **1999**, *17*, 57−61. (b) Trott, O.; Olson, A. J. *J. Comput. Chem.* **2010**, *31*, 455−461.
(23) Cole, P. A.; Shen, K.; Qiao, Y.; Wang, D. *Curr. Opin. Chem. Biol.* **2003**, *7*, 580−585.
(24) (a) For a recent review, see Baruch, A.; Jeffery, D. A.; Bogyo, M. *Trends Cell Biol.* **2004**, *14*, 29−35. (b) Blum, G.; Mullins, S. R.; Keren, K.; Fonovic, M.; Jedeszko, C.; Rice, M. J.; Sloane, B. F.; Bogyo, M. *Nat. Chem. Biol.* **2005**, *1*, 203−209. (c) Blum, G.; von Degenfeld, G.; Merchant, M. J.; Blau, H. M.; Bogyo, M. *Nat. Chem. Biol.* **2007**, *3*, 668−677. (d) Pratt, M. R.; Sekedat, M. D.; Chiang, K. P.; Muir, T. W. *Chem. Biol.* **2009**, *16*, 1001−1012. (e) Watzke, A.; Kosec, G.; Kindermann, M.; Jeske, V.; Nestler, H. P.; Turk, V.; Turk, B.; Wendt, K. U. *Angew. Chem., Int. Ed.* **2008**, *47*, 406−409. (f) Li, J.; Yao, S. Q. *Org. Lett.* **2009**, *11*, 405−408. (g) Hu, M.; Li, L.; Wu, H.; Su, Y.; Yang, P.-Y.; Uttamchandani, M.; Xu, Q.-H.; Yao, S. Q. *J. Am. Chem. Soc.* **2011**, *133*, 12009−12020.
(25) Kim, Y. K.; Lee, J.-S.; Bi, X.; Ha, H.-H.; Ng, S. H.; Ahn, Y.-H.; Lee, J. −J.; Wagner, B. K.; Clemons, P. A.; Chang, Y.-T. *Angew. Chem., Int. Ed.* **2011**, *50*, 2761−2763.
(26) Budin, G.; Yang, K. S.; Reiner, T.; Weissleder, R. *Angew. Chem., Int. Ed.* **2011**, *50*, 9378−9381.
(27) (a) Apsel, B.; Blair, J. A.; Gonzalez, B.; Nazif, T. M.; Feldman, M. E.; Aizenstein, B.; Hoffman, R.; Williams, R. L.; Shokat, K. M.; Knight, Z. A. *Nat. Chem. Biol.* **2008**, *4*, 691−699. (b) Getlik, M.; Grutter, C.; Simard, J. R.; Kluter, S.; Rabiller, M.; Rode, H. B.; Robubi, A.; Rauh, D. *J. Med. Chem.* **2009**, *52*, 3915−3926.
(28) Liu, K.; Kalesh, K. A; Ong, L. B.; Yao, S. Q. *ChemBioChem* **2008**, *9*, 1883−1888.
(29) (a) Vojtechová, M.; Kenigl, F.; Kloncová, E.; Tuhábková, Z. *Arch. Biochem. Biophys.* **2006**, *455*, 136−143. (b) Wang, D.; Cole, P. A. *J. Am. Chem. Soc.* **2001**, *123*, 8883−8886. (c) Osusky, M.; Taylor, S. J.; Shalloway, D. *J. Biol. Chem.* **1995**, *270*, 25729−25732.
(30) (a) Vitolo, O. V.; Sant'Angelo, A.; Costanzo, V.; Battaglia, F.; Arancio, O.; Shelanski, M. *Proc. Natl. Acad. Sci. U.S.A.* **2002**, *99*, 13217−13221. (b) Xing, J.; Kornhauser, J. M.; Xia, Z.; Thiele, E. A.; Greenberg, M. E. *Mol. Cell. Biol.* **1998**, *18*, 1946−1955.
(31) (a) Tao, Z.-F.; et al. *J. Med. Chem.* **2009**, *52*, 6621−6636. (b) Chang, M.; Kanwar, N.; Feng, E.; Siu, A.; Ma, D.; Jongstra, J. *Mol. Cancer Ther.* **2010**, *9*, 2478−2487.
(32) Singh, J.; Petter, R. C.; Baillie, T. A.; Whitty, A. *Nat. Rev. Drug Discovery* **2011**, *10*, 307−317.

(33) Uttamchandani, M.; Lu, C. H. S.; Yao, S. Q. *Acc. Chem. Res.* **2009**, *42*, 1183−1192.
(34) Seeliger, M. A.; Young, M. M.; Henderson, N.; Pellicena, P.; King, D. S.; Falick, A. M.; Kuriyan, J. *Protein Sci.* **2005**, *14*, 3135−3139.
(35) Wu, H.; Ge, J.; Yao, S. Q. *Angew. Chem., Int. Ed.* **2010**, *49*, 6528−6532.
(36) (a) Uttamchandani, M.; Lee, W. L.; Wang, J.; Yao, S. Q. *J. Am. Chem. Soc.* **2007**, *129*, 13110−13117. (b) Uttamchandani, M.; Wang, J.; Li, J.; Hu, M.; Sun, H.; Chen, K. Y. -T.; Liu, K.; Yao, S. Q. *J. Am. Chem. Soc.* **2007**, *129*, 7848−7858.
(37) (a) Gan, C. S.; Guo, T.; Zhang, H.; Kim, S. K.; Sze, S. K. *J. Proteome Res.* **2008**, *7*, 4869−4877. (b) Hao, P.; Guo, T.; Li, X.; Adav, S. S.; Yang, J.; Wei, M.; Sze, S. K. *J. Proteome Res.* **2010**, *9*, 3520−352.